

# Optical and structural properties of sol-gel derived bioactive glasses

AGATA BORSOWSKA<sup>1</sup>, STANISŁAWA SZARSKA<sup>1</sup>, MAREK JASIOŃSKI<sup>2</sup>, KRZYSZTOF MARUSZEWSKI<sup>2</sup>,  
WIESŁAW STRĘK<sup>2</sup>

<sup>1</sup>Institute of Physics, Wrocław University of Technology, Wybrzeże Wyspiańskiego 27,  
50–370 Wrocław, Poland.

<sup>2</sup>Institute of Low Temperature and Structure Research, Polish Academy of Sciences, ul. Okólna 2,  
50–950 Wrocław, Poland.

The preparation of sol-gel derived bioactive glass thin films coated on corundum has been described. Their morphology and physicochemical features were characterized by means of XRD, SEM and UV-VIS-IR methods.

Keywords: biogel, bioactive glass.

## 1. Introduction

The biological response to bioactive glasses made from the CaO–P<sub>2</sub>O<sub>5</sub>–SiO<sub>2</sub> system provides evidence that tissue regeneration is possible, at least in bone. Wheeler's investigations indicate that the use of bioactive gel-glass particles produces an even faster rate of trabecular bone regeneration with no residual gel-glass particles either with high (80%) or low (60%) SiO<sub>2</sub> composition than melt-derived Bioglass<sup>®</sup> [1], [2]. The gel-glass particles resorb more rapidly during the proliferation of trabecular bone. The biological molecules can absorb and desorb from the interconnected pore network without losing their conformation and biological activity. Low-temperature hydrolysis, condensation reactions of tetraethoxysilane (TEOS) and calcium and phosphorus alkoxide precursors create a highly interconnected gel network composed of (SiO<sub>4</sub>)<sub>4</sub>-tetrahedral bonded either to neighboring silica or bridging bonds [3]. The nanometer-scale solid network that comprises the gel is completely interpenetrated by pore liquid. The pore liquid consists of a highly structured hydrated layer that has substantially different physical and chemical properties than free water.

GALLIANO *et al.* [4] developed the method of coating metallic prosthesis with bioactive gel-glasses, YANG *et al.* [5] prepared an organic-inorganic composed material on PMMA. Corundum ceramics surface is not bioactive, which is an obstacle to bonding with living tissues. Therefore, there is an enormous interest in the use of bioactive gel-glasses films coating this ceramics implants, which accelerate the rate of bonding with bone tissues and act as a barrier between the body and corundum

implants. The first investigation connected with sol-gel derived bioactive glasses coatings on corundum porous material was presented by ŁACZKA *et al.*[6].

It is clear that the surface properties must play an important role in bioactivity, and if these surface features can be enhanced through the control of the biogel glass structure, one would expect further improvements in the bioactivity. The main purpose of the present investigation was to study the *in vitro* bioactivity of biogel coating films on corundum. The thin films were characterized by means of XRD, SEM, and UV-VIS-NIR methods.

## 2. Experimental procedures

In agreement with earlier investigations [6], [7] two types of biogel glasses with the nominal compositions are presented in Tab 1.

The basic gel was prepared from the mixture of:  $\text{Si}(\text{OC}_2\text{H}_5)_4$ , (TEOS); calcium nitrate tetrahydrate  $\text{Ca}(\text{NO}_3)_2 \cdot 4\text{H}_2\text{O}$  dissolved in distilled water; triethylphosphate  $\text{OP}(\text{C}_2\text{H}_5\text{O})_3$ ; ethanol  $\text{C}_2\text{H}_5\text{OH}$  as an organic solvent; hydrochloric acid HCl as a catalyst of the reaction of hydrolysis; TritonX-100 as material for lowering of surface tension (B4 sample).

Table 1. Nominal compositions of biogels.

Sample	Nominal composition [mol%]		
	CaO	SiO <sub>2</sub>	P <sub>2</sub> O <sub>5</sub>
A	36	60	4
B4	36	60	4+

The volume ratio of TEOS: $\text{C}_2\text{H}_5\text{OH}$ :HCl was 10:20:0.04 (matrix sample). The basic composition of the gel was prepared from this mixture with the addition of  $\text{Ca}(\text{NO}_3)_2 \cdot 4\text{H}_2\text{O}$  and  $\text{OP}(\text{C}_2\text{H}_5\text{O})_3$  and mixed for about 2 hours.

By the spin-coating method, the coated corundum implant and k9 glass substrates gelation were obtained. This ceramics was produced by Święcki group [9], [10].

Then these films were pulled out from the gel and aged at room temperature for a week. Afterwards these samples were moved into an oven at 80 °C for 24 hours. The dried gels were heated in air at 2 °C/min speed to 450 °C and kept for about 1 hour.

The samples were soaked in simulated body fluid (SBF), an aqueous solution that approximately has the same ion concentration and pH as human blood plasma [8]. This solution was prepared by dissolving reagent grade sodium chloride, sodium bicarbonate, potassium chloride, dibasic potassium phosphate, magnesium chloride, calcium chloride, and sodium sulfate in water, which was buffered at pH 7.3 with hydrochloric acid and aminomethanetrimethanol (Tris). After soaking in SBF for various periods of time, the specimens were removed from solution and dried in air.

In order to examine the microstructures, scanning electron microscopy (model JSM-5800LV JEOL, Japan) observations were conducted. The crystalline structures

were determined by powder X-ray diffraction patterns. XRD patterns were obtained with a diffractometer (Simens D-500) using filtered  $\text{Cu-K}\alpha$  radiation and ICDD database. Microstructure of a sample was examined by an absorbance spectrophotometer (Cary 5E, 2300 UV-VIS-NIR) from 175 to 3300 nm.

### 3. Results and discussion

SEM and EDAX methods in Figs. 1–4 demonstrate the microstructure of films. Figure 1 shows a porous structure of corundum surface. In Fig. 2 we observe an amorphous  $\text{SiO}_2$  layer with small amounts of Ca and P (EDAX analysis), its SEM image of biogel-glass film on corundum. After an exposure to SBF of biogel-glass film, the samples displayed a Ca–P rich structure (Fig. 3), which crystallizes, if the time of SBF soaking is longer (Fig. 4). Silica gel contained many Si–OH groups which are the basis of the nucleation of apatite.

An analysis of the surface layer by an electron microprobe demonstrated the molar ratio Ca/P presented in Tab. 2. These results indicate that with the time of soaking in SBF, the composition of these films is close to that of hydroxyapatite, but after 24 h we obtained one form of the apatites on the crystal layer. We obtained better results for the sample doped by TritonX-100 (B4).

The formation of different types of apatite in synthetic and biological systems is affected by many factors, such as pH, temperature and composition of the system. The

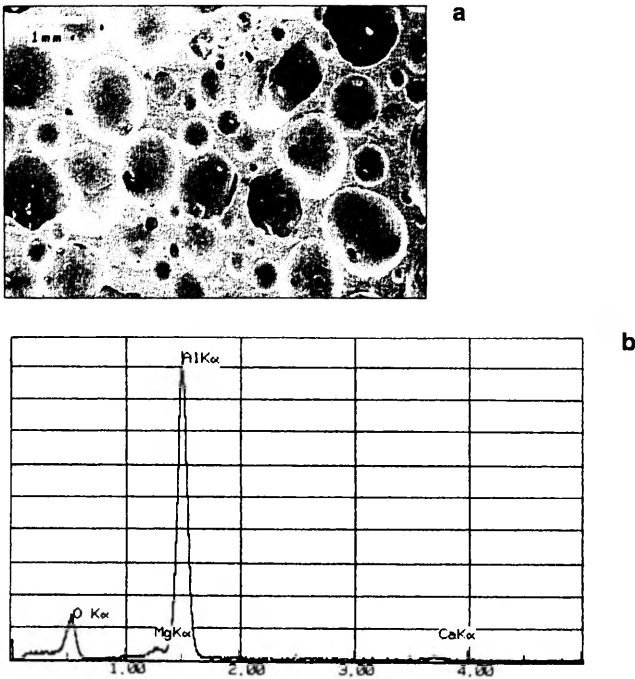


Fig. 1. SEM micrograph (a) and EDAX (b) of porous corundum ceramic.

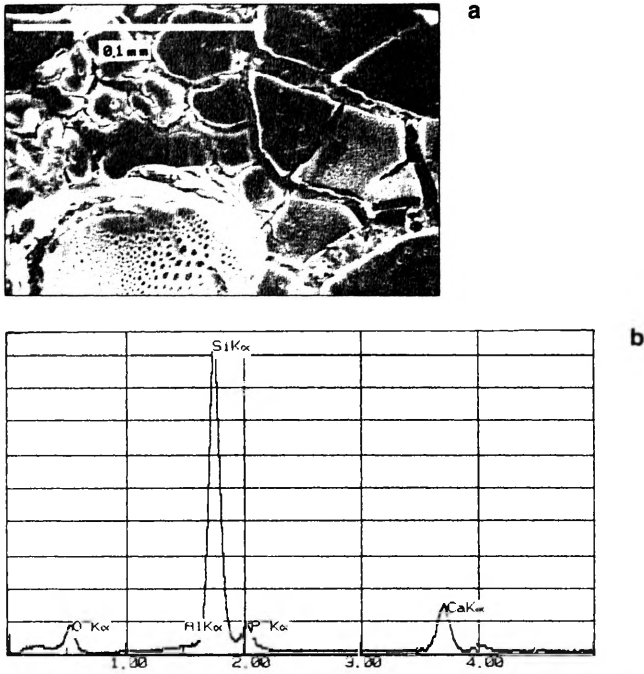


Fig. 2. SEM micrographs (a) and EDAX (b) of biogel-glass A film on corundum.

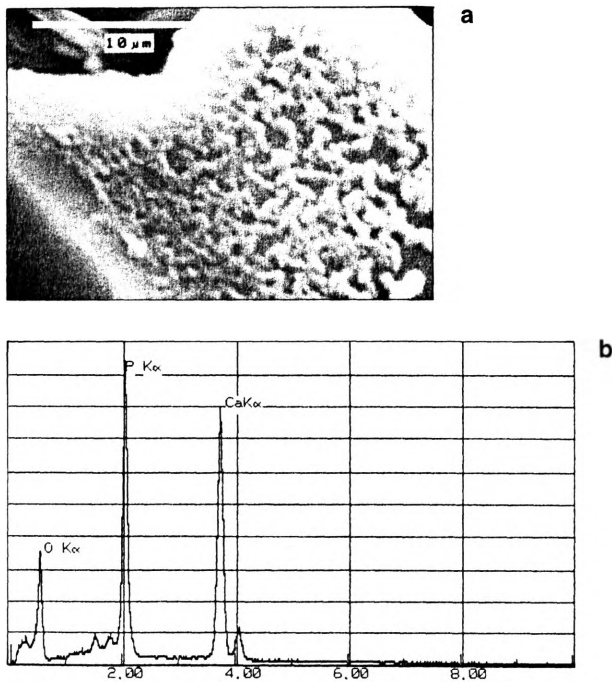


Fig. 3. SEM micrographs (a) and EDAX (b) of biogel-glass A on corundum after 1 h in SBF soaking.

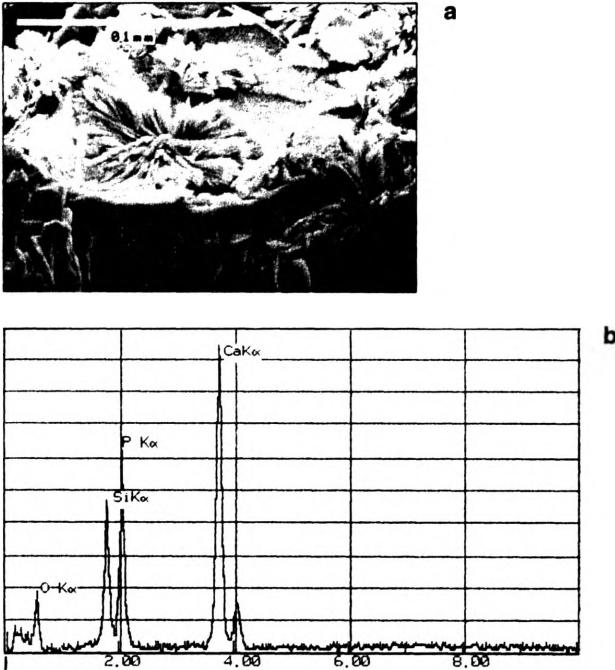


Fig. 4. SEM micrographs (a) and EDAX (b) of biogel-glass A on corundum after 24 h in SBF soaking.

Table 2. Comparison of molar ratio Ca/P for biogel-glass samples.

Samples	Molar ratio Ca/P
Hydroxyapatite as pattern	1.67
Biogel-glass A on corundum soaking of 1 h in SBF	1.08
Biogel-glass A on corundum soaking 24 h w SBF	1.24
Biogel-glass B4 on corundum soaking 24 h w SBF	1.38

compositional factor has more significant effect than pH. No diffraction peaks were observed in the XRD pattern except for a broad band between  $20^\circ$  and  $30^\circ 2\theta$  (in Fig. 5 for A sample), suggesting that, at this stage, the walls were amorphous (these two big peaks at more than  $40^\circ 2\theta$  are the copper lamp peaks). In the same figure we observe some diffraction peaks for biogel-glass sample after 24 h soaking in SBF.

The XRD pattern of the 2nd type of a biogel-glass sample shows five peaks, which from the database match the diffraction pattern of brushite (Fig. 6).

Among calcium phosphates (apatites), at physiological conditions, the thermodynamically most stable form is hydroxyapatite  $\text{Ca}_5(\text{PO}_4)_3(\text{OH})_2$  and only at  $\text{pH} < 5$  the most stable form is  $\text{CaHPO}_4 \cdot 2\text{H}_2\text{O}$  brushite [11].

All the P atoms of hydroxyapatite pertain to  $\text{PO}_4^{3-}$  groups and brushite contains only  $\text{HPO}_4^{2-}$  [12]. The presence of this ion on the surface of apatite would arise from the partial hydrolysis of some  $\text{PO}_4^{3-}$  groups. The hydrolysis process should be

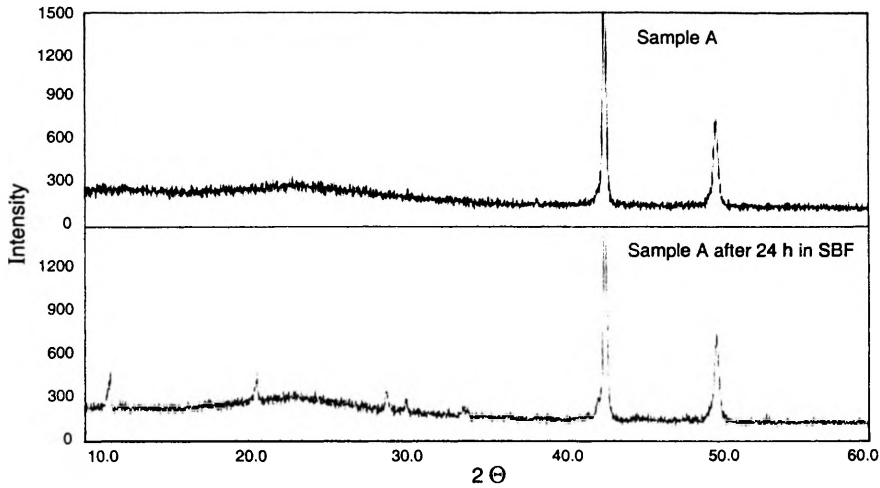


Fig. 5. XRD picture of biogel-glass sample before and after soaking in SBF.

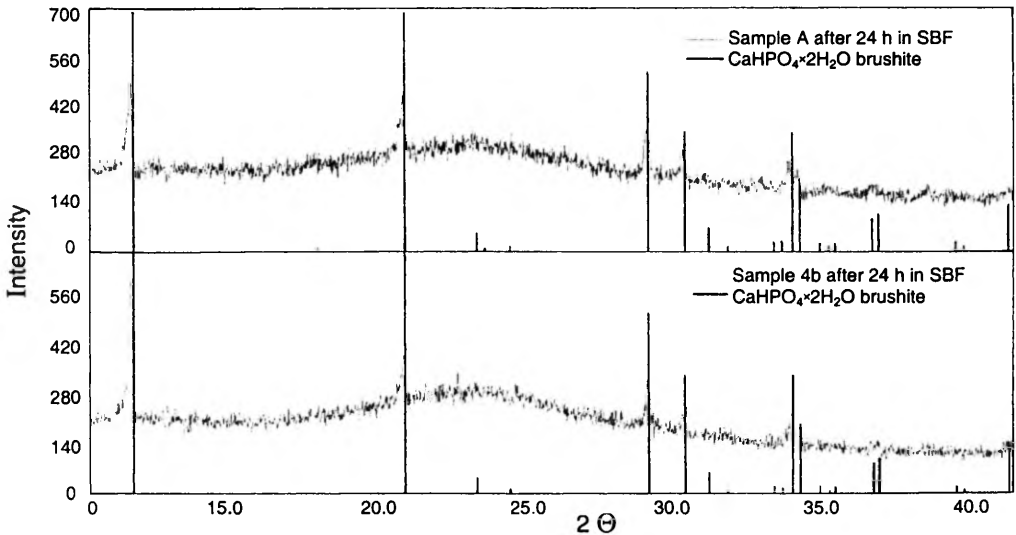


Fig. 6. XRD pattern for the 2nd type of biogel-glass sample – identification of maxima from the database.

associated with the loss of calcium ions in order to keep the charge balanced and, therefore, the molar ratio Ca/P at the surface of the calcium phosphate layer should be lower than that of stoichiometric apatite (Tab. 2).

On the basis of the known mechanism for the formation of apatite, these observations can be explained as follows. In bioactive silica-based glasses, a layer of high-surface-area silica gel is first formed by partial network dissolution and surface polycondensation (Fig. 2). It has been suggested that this silica gel plays a significant

role in apatite formation because the silanol groups present on the surface provide deposition sites for calcium phosphate [3]. One reaction is the interchange between  $\text{Ca}^{2+}$  from the biogel glass and protons from the solution (SBF), which results in an increase in pH value. Another reaction involves the hydrolysis and dissolution of silica, which decreases the pH value. The actual pH depends on the competition between these two reactions. YAN *et al.* [13] demonstrated that in some applications (*e.g.*, bone fillers), the rapid dissolution of the filler, coincident with the replacement by bony tissue, is desired and can be modified by varying the thermal history or the composition of the material.

#### 4. Optical properties

The results presented above suggest that changes in surface structure during the ionic exchange processes are affected by a change in the biogels internal structure. It is reasonable to investigate the structural changes by IR spectroscopy of these gels. There are overtone and combination absorption frequencies in this region, which are different for  $\text{H}_2\text{O}$  and OH groups (in the silanol groups SiOH). It allows us to study, independently, changes in characteristic bands in the IR spectrum occurring during desorption and sorption of  $\text{H}_2\text{O}$  vapor in gels.

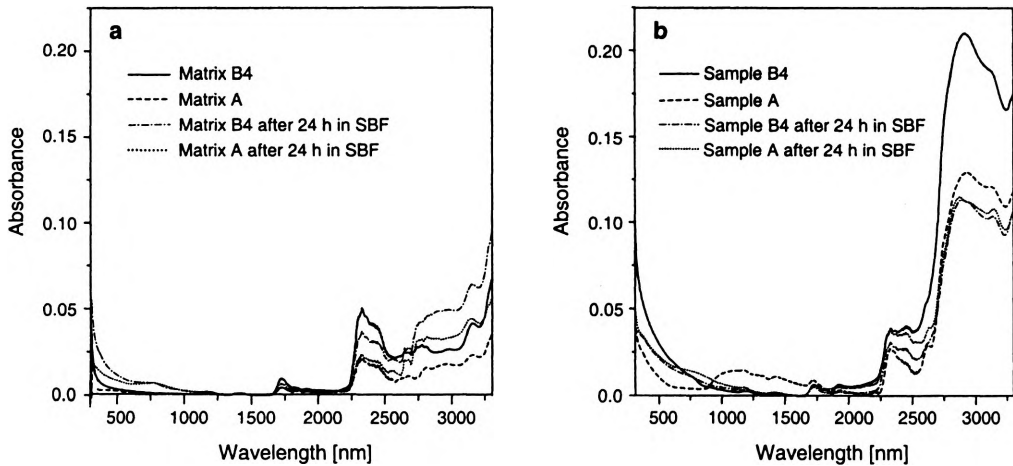


Fig. 7. UV-VIS-NIR absorption spectra of gel (matrix) (a), and biogel-glass A and B4 (b).

In the NIR spectrum (Fig. 7) we note five absorption bands: near 750, 1750, 2250, 2750, and 3250 nm. The absorption band about 2250 nm (present both in Ca-P-free matrix and in biogel glass) probably is connected with the presence of OH group [12]; in agreement with SODOLSKI and KOZŁOWSKI [14], this maximum ( $4340 \text{ cm}^{-1}$ ) points to H-bonded OH. The higher absorbance at a wavelength of 2750 nm for biogel glass than Ca-P-free matrix glass may indicate the presence of P-OH.

## 5. Conclusions

The main conclusions drawn from the presented results can be summarized as follows:

1. Structural investigations show that amorphous biogel glasses were received, while the crystalline brushite grew on their surface as a result of the physiological solution effect.  $\text{HPO}_4^{2-}$  surface groups (present in the brushite) could have a strong influence on the biological processes leading to bone formation brought about by the biomaterial after implantation.

2. Differences in the chemical composition of this layer have been found to be a function of chemical composition of the biogel glass. Changes in optical absorption during the ion exchange processes should be affected by a change in biogel internal surface structure. We have observed that the five absorption bands in the IR spectrum are similar to the energies of Ca-P-free matrix and biogel glass.

## References

- [1] WHEELER D.L., STOKES K.E., [In] *Trans. 23rd Annual Meeting of the Soc. Biomater.*, New Orleans, LA, 1997.
- [2] WHEELER D.L., HOELLRICH R.G., MCLOUGHLIN S.W., CHAMERLAND D.L., STOKES K.E., *Bioceramics* 10, Elsevier, Oxford 1997.
- [3] HENCH L.L., *Biomaterials* 19 (1998), 1419.
- [4] GALLIANO P., DE DAMBORENEA J.J., PASQUAL M.J., DURAN A., *J. Sol-Gel Sci. Technol.* 13 (1998), 723.
- [5] YANG J.M., LU C.S., HSU Y.G., SHIH C.H., *J. Biomed. Mater. Res.* 38 (1997), 143.
- [6] ŁACZKA M., JAEGERMANN Z., CHOLEWA K., CIOŁEK L., *Szkło i Ceramika*, 1 (1996), 14 (in Polish).
- [7] PEREIRA M.M., CLARK A.E., HENCH L.L., *J. Biomed. Mater. Res.* 28 (1994), 693.
- [8] KOKUBO T., *J. Non-Cryst. Solids* 120 (1990), 138.
- [9] ROSIEK G., MIKSIEWICZ C., BIENIEK J., *Szkło i Ceramika* 25 (1984), 41 (in Polish).
- [10] ŚWIĘCKI Z., *Bioceramics for Orthopedics*, IPPT PAN, Warszawa, 1992 (in Polish).
- [11] LUSVARDI G., MENABUE L., SALADINI M., [In] *Materials in Clinical Applications*, [Ed.] P. Vincenzini, Techna Srl, 1995, p. 35.
- [12] ONG J.L., LUCAS L.C., RAIKAR G.N., WEIRMAR J.J., GREGORY J.C., *Colloids Surf. A* 87 (1994), 151.
- [13] YAN H., ZHANG K., BLANFORD CH.F., FRANCIS L.F., STEIN A., *Chem. Mater.* 13 (2001), 1374.
- [14] SODOLSKI H., KOZŁOWSKI M., *J. Non-Cryst. Solids* 194 (1996), 241.

*Received September 26, 2002*